

Static and Vibrational Properties of Equiatomic Cesium-Alkali Binary Alloys

Aditya M. Vora*

Humanities and Social Science Department, S. T. B. S. College of Diploma Engineering, Shri Swami Atmanand Sarswati Vidya Sankul, Opp. Kapodra Police Station, Varachha Road, Surat 395 006, Gujarat, India

(Received 01 March 2012; published online 04 July 2012)

The computations of the static and vibrational properties of four equiatomic Cs-based binary alloys viz. $\text{Cs}_{0.5}\text{Li}_{0.5}$, $\text{Cs}_{0.5}\text{Na}_{0.5}$, $\text{Cs}_{0.5}\text{K}_{0.5}$ and $\text{Cs}_{0.5}\text{Rb}_{0.5}$ to second order in local model potential is discussed in terms of real-space sum of Born von Karman central force constants. The local field correlation functions due to Hartree (H), Ichimaru-Utsumi (IU) and Sarkar *et al.* (S) are used to investigate influence of the screening effects on the aforesaid properties. Results for the lattice constants, i.e. C_{11} , C_{12} , C_{44} , $C_{12} - C_{44}$, C_{12} / C_{44} , and bulk modulus B obtained using the H-local field correction function, have higher values in comparison with the results obtained for the same properties using IU and S local field correction functions. The results for the Shear modulus (C'), deviation from Cauchy's relation, Poisson's ratio σ , Young modulus Y , propagation velocity of elastic waves, phonon dispersion curves and degree of anisotropy A are highly appreciable for the four equiatomic Cs-based binary alloys.

Keywords: Static and vibrational properties, Cs-based equiatomic alloys, Phonon dispersion curves (PDC).

PACS numbers: 62.30. + d; 62.20. - x; 62.20.Dc; 63.50. + x

1. INTRODUCTION

In the study of various properties of solids, one frequently requires the knowledge of interaction energy between the ions or atoms. The studies of a pair-effective interionic interaction in simple metals have long history and originally they were not systematized and were concerned with individual metals on groups of metals. In recent years, considerable attention has been devoted to the theoretical study of the nature of effective interaction between constituent atom or ion in simple metals and their alloys [1-11]. The bcc $A_{1-x}B_x$ ($A = \text{Cs}$; $B = \text{Li}, \text{Na}, \text{K}, \text{Rb}$) alloy system forms substitutional solid solution for the entire region of concentration 'x' of the second component, and the crystal binding of the solid solution is unchanged compared with that of the pure alkali metals. Theoretical studies about the lattice dynamics of the alloy systems have been devoted to $\text{Cs}_{0.5}\text{Li}_{0.5}$, $\text{Cs}_{0.5}\text{Na}_{0.5}$, $\text{Cs}_{0.5}\text{K}_{0.5}$ and $\text{Cs}_{0.5}\text{Rb}_{0.5}$ systems since the lattice dynamics of the pure alkalis has been investigated in detail. But the work on the comprehensive study of static and vibrational properties their binary alloys is almost negligible [1-10]. Only Soma *et al.* [10] have studied the phonon dispersion curves of $\text{Cs}_{0.7}\text{K}_{0.3}$, $\text{Cs}_{0.7}\text{Rb}_{0.3}$, $\text{Cs}_{0.3}\text{Rb}_{0.7}$ and $\text{Rb}_{0.71}\text{Cs}_{0.29}$ alloys. Very recently we have reported the static and vibrational properties of some alkali metals and their equiatomic binary alloys using model potential formalism [1-8]. Also, Gajjar *et al.* [9] have studied the lattice dynamics of bcc $\text{Cs}_{0.3}\text{K}_{0.7}$ alloy. Experimentally, Kamitakahara and Copley [12] have studied the lattice dynamics of $\text{Rb}_{1-x}\text{K}_x$ alloys with $x = 0.06, 0.18$ and 0.29 by neutron scattering. Recently, Chushak and Baumketner [13] have reported the dynamical properties of liquid $\text{Cs}_{0.3}\text{K}_{0.7}$ alloy. Most of the earlier theoretical studies are used various types of local as well as non-local model potential with older local field correction function. Lattice dynamics of $\text{Rb}_{71}\text{K}_{29}$ binary alloys has been studied by Jacucci *et al.* [14] using MD technique. Also, the equiatomic alloys of alkali metals contain equal

amount of volume, valence and the Fermi energy, which is reflected the nature of the alloying behaviour.

As a consequence of the disorder, the phonon spectra of alloys can differ considerable in character from those of the pure metals. Localized vibrational modes may be present, and all phonons acquire a broadening and shift in frequency. Besides their importance for the thermodynamic properties, the lattice vibrations in alloy systems provide an ideal testing ground for any theory of elementary excitations in disordered systems because the energy wave vector relationship can be measured directly by either the coherence inelastic neutron scattering experimentally or by the many theoretical models. Once the phonon spectrum of the alloy is known, the calculation of the vibrational contribution to the thermodynamic functions is straightforward [15].

Therefore, in the present article, we have decided to work on four equiatomic Cs-based binary alloys i.e. $\text{Cs}_{0.5}\text{Li}_{0.5}$, $\text{Cs}_{0.5}\text{Na}_{0.5}$, $\text{Cs}_{0.5}\text{K}_{0.5}$ and $\text{Cs}_{0.5}\text{Rb}_{0.5}$ with PAA model [1-9]. Well known single parametric local model potential of Gajjar *et al.* [9] is used to describe the electron-ion interaction. For the first time an advanced and more recent local field correlation functions due to Ichimaru-Utsumi (IU) [16] and Sarkar *et al.* [17] has been employed in such investigations. This helps in identifying the influence of exchange and correlation effects in the static form of Hartree (H) dielectric function [18]. $\text{Cs}_{0.5}\text{Li}_{0.5}$, $\text{Cs}_{0.5}\text{Na}_{0.5}$, $\text{Cs}_{0.5}\text{K}_{0.5}$ and $\text{Cs}_{0.5}\text{Rb}_{0.5}$ with PAA model [1-9]. Well known single parametric local model potential of Gajjar *et al.* [9] is used to describe the electron-ion interaction. For the first time an advanced and more recent local field correlation functions due to Ichimaru-Utsumi (IU) [16] and Sarkar *et al.* [17] has been employed in such investigations. This helps in identifying the influence of exchange and correlation effects in the static form of Hartree (H) dielectric function [18].

* voraam@yahoo.com

2. THEORETICAL METHODOLOGY

The phonon frequencies can be obtained by solving the standard secular determinantal equation [1-11]

$$\det|D_{\alpha\beta}(q) - 4\pi^2\nu^2 M \delta_{\alpha\beta}| = 0, \quad (1)$$

where, M is the ionic mass, ν the phonon frequency and $D_{\alpha\beta}(q)$ the dynamical matrix in which the force between two ions depends only upon the distance between them is given by,

$$D_{\alpha\beta}(q) = \sum_n (1 - e^{i\mathbf{q}\cdot\mathbf{r}}) \left. \frac{d^2\Phi(r)}{dr_\alpha dr_\beta} \right|_{r=r_n}, \quad (2)$$

where $\Phi(r)$ is the interionic pair potential, and r_α and r_β are α^{th} and β^{th} Cartesian components of the position vector of n^{th} ion, respectively.

The interionic pair potential $\Phi(r)$ is computed from the well known relation [1-11]

$$\Phi(r) = \frac{Z^2 e^2}{r} + \frac{\Omega_0}{\pi^2} \int F(q) \frac{\sin qr}{qr} dq. \quad (3)$$

Where $F(q)$ is the energy wave number characteristic given by [1-11]

$$F(q) = \frac{\Omega_0 q^2}{8\pi e^2} |W_B(q)|^2 \frac{[\varepsilon_H(q) - 1]}{1 + [\varepsilon_H(q) - 1][1 - f(q)]}. \quad (4)$$

With Ω_0 , $W_B(q)$, $\varepsilon_H(q)$ and $f(q)$ are the atomic volume, bare-ion pseudopotential, static Hartree dielectric function and local field correlation function, respectively.

The bare-ion pseudopotential due to Gajjar *et al.* [9] is given by

$$W_B(q) = \frac{-8\pi Z}{\Omega_0 q^2} \left(\cos(qr_C) - \frac{(qr_C)^2}{(1 + (qr_C)^2)} \right). \quad (5)$$

here, Z and r_C are the valence and parameter of the model potential, respectively. The details of the model potential are narrated in the literature [9]. In the present investigation, the local field correction functions due to H, IU and S are incorporated to see the impact of exchange and correlation effects. The details of all the local field corrections are below.

The H-screening function [18] is purely static, and it does not include the exchange and correlation effects. The expression of it is,

$$f(X) = 0 \quad (6)$$

The Ichimaru-Utsumi (IU)-local field correction function [16] is a fitting formula for the dielectric screening function of the degenerate electron liquids at metallic and lower densities, which accurately reproduces the Monte-Carlo results as well as it also, satisfies the self consistency condition in the compressibility sum rule and short range correlations. The fitting formula is

$$f(X) = A_{IU} Q^4 + B_{IU} Q^2 + C_{IU} + \left[A_{IU} Q^4 + \left(B_{IU} + \frac{8A_{IU}}{3} \right) Q^2 - C_{IU} \right] \times$$

$$\times \left\{ \frac{4 - Q^2}{4Q} \ln \left| \frac{2 + Q}{2 - Q} \right| \right\} \quad (7)$$

Sarkar *et al.* (S) [17] have proposed a simple form of local field correction function on the basis of IU-local field correction function [16], which is of the form

$$f(X) = A_S \{ 1 - (1 + B_S Q^4) \exp(-C_S Q^2) \}. \quad (8)$$

Where $Q = 2X$. The parameters A_{IU} , B_{IU} , C_{IU} , A_S , B_S and C_S are the atomic volume dependent parameters of IU and S-local field correction functions. The mathematical expressions of these parameters are narrated in the respective papers of the local field correction functions [16, 17].

The dynamical matrix element used in the present calculation finally takes the form,

$$D_{\alpha\beta}(q) = \sum_n (1 - e^{i\mathbf{q}\cdot\mathbf{r}}) \left[K_t + \frac{r_\alpha r_\beta}{r^2} (K_r - K_t) \right], \quad (9)$$

Here K_t and K_r are the force constants between a pair of ions interacting through a central interaction and n specifies shell index.

$$K_t = \frac{1}{r} \frac{d\Phi(r)}{dr} = -\frac{Z^2 e^2}{r^3} + \frac{\Omega_0}{\pi^2 r^2} \int_0^\infty F(q) q^2 \left[\cos(qr) - \frac{\sin(qr)}{qr} \right] dq. \quad (10)$$

$$K_r = \frac{d^2\Phi}{dr^2} = \frac{2Z e^2}{r^3} + \frac{\Omega_0}{\pi^2 r^2} \int_0^\infty F(q) q^2 \left[\frac{2\sin(qr)}{qr} - 2\cos(qr) - qr \sin(qr) \right] dq. \quad (11)$$

Using these atomic force constants, we can generate inter atomic force constants $K_{\alpha\beta}$ which can then be employed to investigate the elastic constants

$$K_{\alpha\beta} = \frac{d^2\Phi(r)}{dr_\alpha dr_\beta} = \left[\delta_{\alpha\beta} - \frac{r_\alpha r_\beta}{r^2} \right] K_t + \frac{r_\alpha r_\beta}{r^2} K_r. \quad (12)$$

Under the long-wave phonon method, the elastic constants are studied by [1-11]

$$C_{11} = \frac{1}{12a} \sum_n N(n) \left[x^2 K_{xx}^n + y^2 K_{yy}^n + z^2 K_{zz}^n \right], \quad (13)$$

$$C_{44} = \frac{1}{24a} \sum_n N(n) \times \left[(y^2 + z^2) K_{xx}^n + (z^2 + x^2) K_{yy}^n + z^2 K_{zz}^n \right], \quad (14)$$

$$C_{12} + C_{44} = \frac{1}{6a} \sum_n N(n) \left[yz K_{yz}^n + zx K_{zx}^n + xy K_{xy}^n \right]. \quad (15)$$

Where " a " is the lattice constant and $N(n)$ is the number of atoms at the n^{th} neighbour separation. The shear modulus C and bulk modulus B are given by [1-11]

$$C' = [(C_{11} - C_{12})/2]. \quad (16)$$

and

$$B = [(C_{11} + 2C_{12})/3]. \quad (17)$$

The extent to which the interatomic forces are non-pair wise can be obtained by investigating the breakdown of the Cauchy relation. The Cauchy's ratio is obtained by C_{12}/C_{44} .

Poisson's ratio σ is the second independent elastic parameter and is given as [1-8],

$$\sigma = C_{12}/(C_{11} + C_{12}). \quad (18)$$

From the calculated values of the bulk modulus and Poisson's ratio, Young modulus Y is derived as [1-11],

$$Y = 3B(1 - 2\sigma). \quad (19)$$

In the cubic system the propagation velocity of longitudinal and transverse waves in [100], [110] and [111] directions are given as [1-11]

$$v_L[100] = [C_{11}/\rho]^{1/2}. \quad (20)$$

$$v_L[110] = [(C_{11} + C_{12} + 2C_{44})/2\rho]^{1/2}. \quad (21)$$

$$v_L[111] = [(C_{11} + 2C_{12} + 4C_{44})/3\rho]^{1/2}. \quad (22)$$

$$v_T[100] = v_{T1}[110] = [C_{44}/\rho]^{1/2}. \quad (23)$$

$$v_{T2}[110] = [(C_{11} - C_{12})/2\rho]^{1/2}. \quad (24)$$

$$v_T[111] = [(C_{11} - C_{12} + 2C_{44})/3\rho]^{1/2}. \quad (25)$$

The behavior of phonon frequencies in the limit independent of direction is given by [1-11]

$$Y_1 = \lim_{q \rightarrow 0} \sum_i \frac{\omega_i^2(q)}{q^2} = \left[\frac{(C_{11} + 2C_{44})}{\rho} \right], \quad (26)$$

and

$$Y_2 = \lim_{q \rightarrow 0} \left(\frac{\omega_{T1}}{\omega_{T2}} \right)^2 = \left[\frac{(C_{11} - C_{12})}{2C_{44}} \right]. \quad (27)$$

The degree of elastic anisotropy A is the inverse of Y_2 , i.e. [1-11],

$$A = [2C_{44}/(C_{11} - C_{12})]. \quad (28)$$

The value of A is unity when the material is elastically isotropic and differs from unity otherwise.

3. RESULTS AND DISCUSSION

Constants and parameters employed for the present computational study are listed in Table 1. In evaluating integration in Eqs. (10) and (11) the upper limit of integral is taken as $40 k_F$ so that, a complete convergence of the model potential is achieved at higher momentum

transfer and it covers all the oscillations of the form factor. Therefore, any artificial/fictitious cut-off in the present computations is avoided. In the present computation, the error associated will be of the order of $10^{-6} k_F / 2$. We have performed the real space sum analysis in r-space of 33 sets of nearest neighbours, which are found sufficient for computing the elastic constants and bulk modulus using interatomic force constants and for considering a long-range character for proper convergence of the calculation and to achieve desired accuracy. The present model is valid for both ordered and disordered alloys [1-8].

Table 1 – Input parameters and other constants

Metal	Z	k_F (au)	Ω_0 (au) ³	rc (au)
Li	1	0.5890	144.9	0.7738
Na	1	0.4882	254.5	1.0765
K	1	0.3947	481.4	1.3880
Rb	1	0.3693	587.9	1.4837
Cs	1	0.3412	745.5	1.9108

In the present computation, the bcc crystal structure considered for all the solid solutions. The lattice constants " a " are obtained from the well known relation $(2\Omega_0)^{1/3}$. Tables 2-5 display the computed values of some static and vibrational properties of four equiatomic Cs-based binary alloys. It is noted in Tables 2-5 that our results for C_{11} , C_{12} , C_{44} , $C_{12} - C_{44}$, C_{12}/C_{44} and bulk modulus B from H-local field correction function give values higher than those obtained for the IU and S-local field correction functions. There is a good agreement for the calculated values of the Shear modulus C' , deviation from Cauchy's relation, Poisson's ratio σ , Young modulus Y , propagation velocity of elastic waves, phonon dispersion curves (PDC) and degree of anisotropy A using H, IU and S-local field correction functions.

Table 2 – Static and vibrational properties of Cs_{0.5}Li_{0.5} alloy

Properties	H	IU	S
C_{11} in 10^{10} dyne-cm ⁻²	8.01	6.73	5.76
C_{12} in 10^{10} dyne-cm ⁻²	7.33	5.61	5.11
C_{44} in 10^{10} dyne-cm ⁻²	2.99	3.76	2.74
C' in 10^9 dyne-cm ⁻²	3.40	5.56	3.25
B in 10^{10} dyne-cm ⁻²	7.56	5.99	5.32
$(C_{12} - C_{44})$ in 10^{10} dyne-cm ⁻²	4.34	1.86	2.37
Cauchy's ratio (C_{11} / C_{44})	2.45	1.49	1.86
σ	0.48	0.45	0.47
Y in 10^{10} dyne-cm ⁻²	1.00	1.62	0.96
v_L [100] in 10^5 cm-sec ⁻¹	2.13	1.95	1.81
v_T [100] in 10^5 cm-sec ⁻¹	1.30	1.46	1.25
v_L [110] in 10^5 cm-sec ⁻¹	2.46	2.37	2.15
v_{T1} [110] in 10^5 cm-sec ⁻¹	1.30	1.46	1.25
v_{T2} [110] in 10^5 cm-sec ⁻¹	0.44	0.56	0.43
v_L [111] in 10^5 cm-sec ⁻¹	2.56	2.50	2.26
v_T [111] in 10^5 cm-sec ⁻¹	0.83	0.96	0.80
Y_1 in 10^{10} dyne-cm ⁻²	7.95	8.09	6.38
Y_2	0.11	0.15	0.12
A	8.81	6.76	8.43

Table 3 – Static and vibrational properties of Cs_{0.5}Na_{0.5} alloy

Properties	H	IU	S
C_{11} in 10^{10} dyne-cm ⁻²	8.15	5.87	5.95
C_{12} in 10^{10} dyne-cm ⁻²	7.53	5.09	5.37
C_{44} in 10^{10} dyne-cm ⁻²	2.44	2.38	2.30
C' in 10^9 dyne-cm ⁻²	3.08	3.96	2.89
B in 10^{10} dyne-cm ⁻²	7.74	5.36	5.56
$(C_{12} - C_{44})$ in 10^{10} dyne-cm ⁻²	5.09	2.72	3.08
Cauchy's ratio (C_{11} / C_{44})	3.08	2.14	2.34
σ	0.48	0.46	0.47
Y in 10^{10} dyne-cm ⁻²	0.91	1.16	0.85
v_L [100] in 10^5 cm-sec ⁻¹	2.16	1.84	1.85
v_T [100] in 10^5 cm-sec ⁻¹	1.18	1.17	1.15
v_L [110] in 10^5 cm-sec ⁻¹	2.43	2.12	2.13
v_{T1} [110] in 10^5 cm-sec ⁻¹	1.18	1.17	1.15
v_{T2} [110] in 10^5 cm-sec ⁻¹	0.42	0.48	0.41
v_L [111] in 10^5 cm-sec ⁻¹	2.51	2.21	2.22
v_T [111] in 10^5 cm-sec ⁻¹	0.76	0.78	0.74
Y_1 in 10^{10} dyne-cm ⁻²	7.46	6.09	6.03
Y_2	0.13	0.17	0.13
A	7.93	6.00	7.94

Table 4 – Static and vibrational properties of Cs_{0.5}K_{0.5} alloy

Properties	H	IU	S
C_{11} in 10^{10} dyne-cm ⁻²	6.87	4.92	4.86
C_{12} in 10^{10} dyne-cm ⁻²	6.35	4.33	4.40
C_{44} in 10^{10} dyne-cm ⁻²	1.95	1.96	1.79
C' in 10^9 dyne-cm ⁻²	2.61	2.93	2.32
B in 10^{10} dyne-cm ⁻²	6.52	4.53	4.55
$(C_{12} - C_{44})$ in 10^{10} dyne-cm ⁻²	4.40	2.38	2.61
Cauchy's ratio (C_{11} / C_{44})	3.26	2.21	2.46
σ	0.48	0.47	0.47
Y in 10^{10} dyne-cm ⁻²	0.77	0.86	0.68
v_L [100] in 10^5 cm-sec ⁻¹	2.09	1.77	1.76
v_T [100] in 10^5 cm-sec ⁻¹	1.11	1.12	1.07
v_L [110] in 10^5 cm-sec ⁻¹	2.33	2.05	2.02
v_{T1} [110] in 10^5 cm-sec ⁻¹	1.11	1.12	1.07
v_{T2} [110] in 10^5 cm-sec ⁻¹	0.41	0.43	0.38
v_L [111] in 10^5 cm-sec ⁻¹	2.41	2.13	2.10
v_T [111] in 10^5 cm-sec ⁻¹	0.72	0.73	0.69
Y_1 in 10^{10} dyne-cm ⁻²	6.85	5.62	5.36
Y_2	0.13	0.15	0.13
A	7.47	6.66	7.70

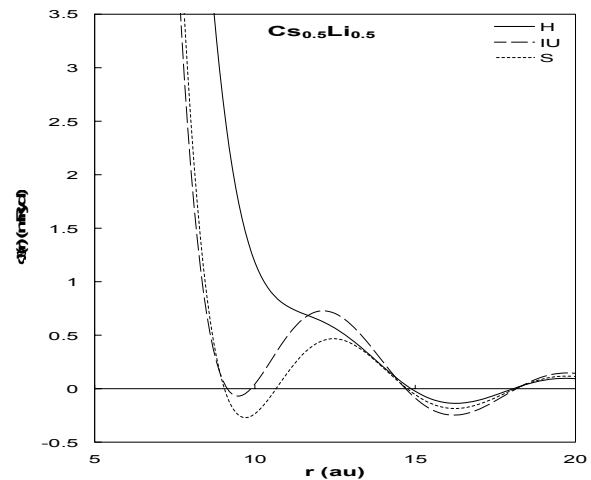
Table 5 – Static and vibrational properties of Cs_{0.5}Rb_{0.5} alloy

Properties	H	IU	S
C_{11} in 10^{10} dyne-cm ⁻²	6.04	4.26	4.29
C_{12} in 10^{10} dyne-cm ⁻²	5.59	3.77	3.88
C_{44} in 10^{10} dyne-cm ⁻²	1.74	1.77	1.60
C' in 10^9 dyne-cm ⁻²	2.26	2.43	2.05
B in 10^{10} dyne-cm ⁻²	5.74	3.93	4.02
$(C_{12} - C_{44})$ in 10^{10} dyne-cm ⁻²	3.84	2.00	2.29
Cauchy's ratio (C_{11} / C_{44})	3.20	2.13	2.43
σ	0.48	0.47	0.47
Y in 10^{10} dyne-cm ⁻²	0.67	0.71	0.60
v_L [100] in 10^5 cm-sec ⁻¹	1.81	1.52	1.53
v_T [100] in 10^5 cm-sec ⁻¹	0.97	0.98	0.93
v_L [110] in 10^5 cm-sec ⁻¹	2.03	1.77	1.76
v_{T1} [110] in 10^5 cm-sec ⁻¹	0.97	0.98	0.93

Properties	H	IU	S
v_{T2} [110] in 10^5 cm-sec ⁻¹	0.35	0.36	0.33
v_L [111] in 10^5 cm-sec ⁻¹	2.10	1.86	1.83
v_T [111] in 10^5 cm-sec ⁻¹	0.63	0.64	0.60
Y_1 in 10^{10} dyne-cm ⁻²	5.19	4.24	4.08
Y_2	0.13	0.14	0.13
A	7.73	7.29	7.80

It is noticed from the present study that, the percentile influence of the IU-local field correction function with respect to the static H-local field correction function on the vibrational properties of Cs_{0.5}Li_{0.5}, Cs_{0.5}Na_{0.5}, Cs_{0.5}K_{0.5} and Cs_{0.5}Rb_{0.5} is found to be 1.76 %-63.53 %, 0.85 %-46.56 %, 0.51 %-45.91 % and 1.59 %-33.44 %, respectively. Such influence of the S-local field correction function with respect to the static H-local field correction function on the vibrational properties is as follows: for Cs_{0.5}Li_{0.5} is 2.27 %-30.29 %, for Cs_{0.5}Na_{0.5} is 2.08 %-39.49 %, for Cs_{0.5}K_{0.5} is 0 %-40.68 % and for Cs_{0.5}Rb_{0.5} is 0 %-40.36 %. This clearly indicates that the local field correlations play a very effective role in explaining correctly the static and dynamic properties of such solid solutions.

The interionic pair potentials $\Phi(r)$ computed from the three local field correction functions are displayed in Figures 1-4 for four equiatomic Cs-based binary alloys. We have seen from Figure 1 that, the well depth is slightly increasing due to influence of IU and S screening functions in compared to H-screening. The first zero position $V(r=r_0)$ of interionic pair potentials of Cs_{0.5}Li_{0.5} alloy due to H, IU and S functions occurs at $r_0 \approx 15.8$ au, 8.3 au and 8.3 au, respectively. The presently generated interionic pair potentials of Cs_{0.5}Na_{0.5} alloy are displayed in Figure 2. The first zero for $V(r=r_0)$ due to H, IU and S functions occurs at $r_0 \approx 16.1$ au, 9.5 au and 9.5 au, respectively. The presently calculated interionic pair potentials of Cs_{0.5}K_{0.5} alloy are observed in Figure 3. The position of interionic pair potentials at $r=r_0$ due to H-function occurs at $r_0 = 17.8$ au, while influence of IU and S screenings enhances this zero slightly and occurs at $r_0 \leq 10.6$ au. The first zero position of interionic pair potentials at $r=r_0$ of Cs_{0.5}Rb_{0.5} at $r=r_0$ due to H, IU and S functions occurs at $r_0 \approx 18.2$ au, 11.8 au and 11.8 au, respectively.

**Fig. 1** – Interionic pair potential of Cs_{0.5}Li_{0.5} alloy

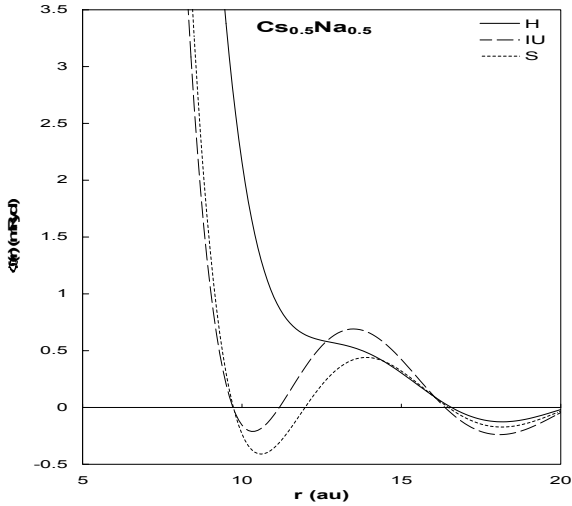


Fig. 2 – Interionic pair potential of $\text{Cs}_{0.5}\text{Na}_{0.5}$ alloy

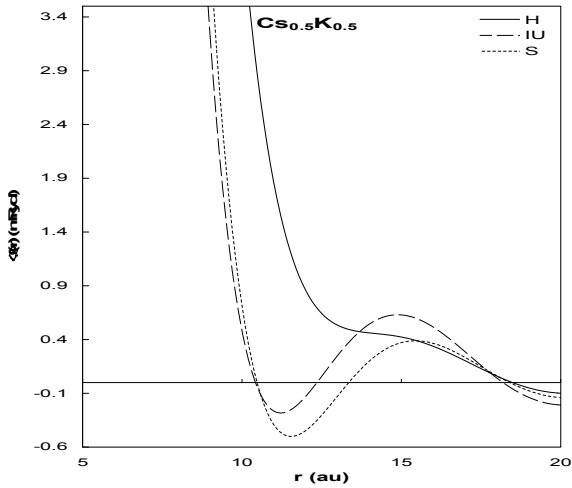


Fig. 3 – Interionic pair potential of $\text{Cs}_{0.5}\text{K}_{0.5}$ alloy

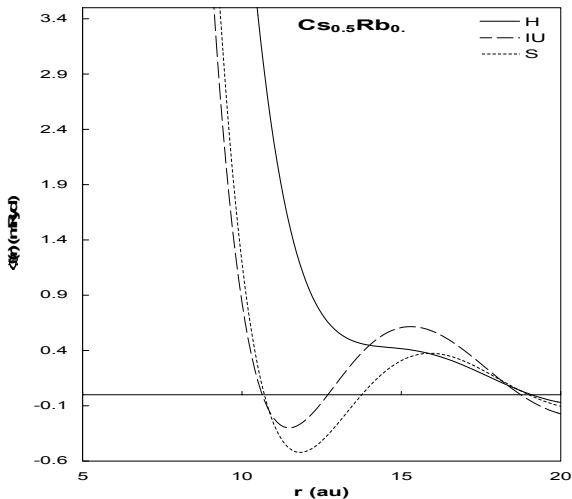


Fig. 4 – Interionic pair potential of $\text{Cs}_{0.5}\text{Rb}_{0.5}$ alloy

Also, we have observed from Figures 1-4 that, the inclusion of screening functions hardly changes the nature of the pair potentials, except around the first minimum. Thus, the inclusion of exchange and correlations on the $V(r=r_0)$ is substantial. The pair potential

due to IU-screening function is lying between those of H- and S-screening function. The results of the interionic pair potentials show significant oscillations and potential energy remains positive in the larger r -region.

Thus, the Coulomb repulsive potential part dominates the oscillations due to ion-electron-ion interactions. Most of the interionic pair potential curves of four equiatomic Cs-based binary alloys show hardcore nature. Also, we observed from the interionic pair potential curves that, when we move from $\text{Cs}_{0.5}\text{Li}_{0.5} \rightarrow \text{Cs}_{0.5}\text{Rb}_{0.5}$ alloys, the depth of the interionic pair potential increases with increase in the average volume of the solid alloys. But the well width increases compared to H-screening. The maximum depth in the interionic pair potentials is obtained for S-function. The interionic pair potentials obtained from Eq. (3) is then used in the computations of the lattice dynamics of the Cs-based binary alloys.

A good description of Cs or Rb is rather more complicated than that of the other alkali elements. The problem stems from the fact that at pure Cs or Rb density the compressibility of the electron gas is close to zero, and is conceivably negative. Hence, the normal pseudopotential perturbation approach based on the electron gas as the zero order approximation is rather dubious. This is because one is starting with a thermodynamically unstable system to provide a description of one which is thermodynamically stable. The way out of this dilemma, was used to scale the electron gas density parameter i.e. the Wigner-Seitz radius r_s by the band structure effective mass m^* , which then meant that one was dealing with an effective density for which the electron gas compressibility was large and positive. The physical meaning of this approach was not clear, but it bears a close resemblance to that the effect of large core polarization of Cs or Rb could be taken into account by a suitable scaling of r_s , also in the direction of large, positive compressibility [13]. But, in the present results of the lattice dynamics of the equiatomic Cs-based binary alloys, we have made straightforward computation without any assumptions.

We have also studied the PDC of four equiatomic Cs-based binary alloys viz. $\text{Cs}_{0.5}\text{Li}_{0.5}$, $\text{Cs}_{0.5}\text{Na}_{0.5}$, $\text{Cs}_{0.5}\text{K}_{0.5}$ and $\text{Cs}_{0.5}\text{Rb}_{0.5}$ along [100], [110] and [111] directions of high symmetry, which are displayed in Figures 5-8. We have found that the phonon frequencies in the longitudinal branch (L) are more sensitive to the exchange and correlation effects in comparison with the transverse branches (T_1 and T_2).

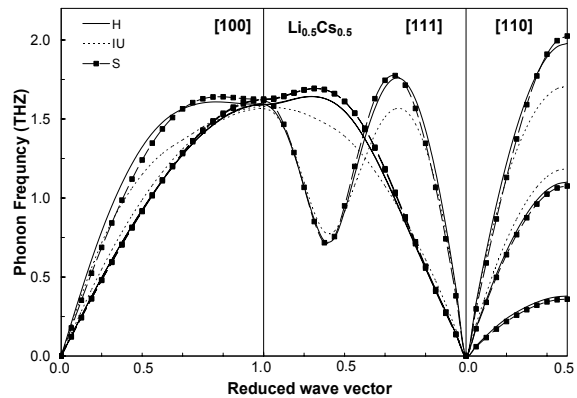
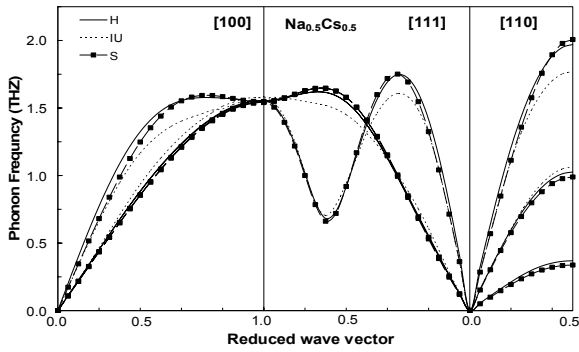
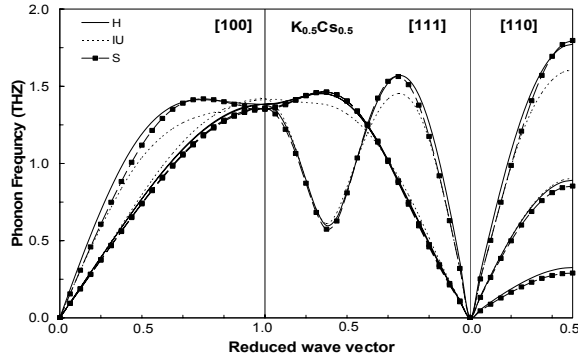
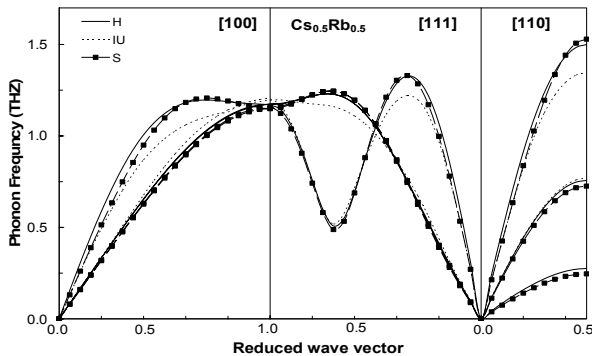


Fig. 5 – Phonon dispersion curves of $\text{Cs}_{0.5}\text{Li}_{0.5}$ alloy

Fig. 6 – Phonon dispersion curves of $\text{Cs}_{0.5}\text{Na}_{0.5}$ alloyFig. 7 – Phonon dispersion curves of $\text{Cs}_{0.5}\text{K}_{0.5}$ alloyFig. 8 – Phonon dispersion curves of $\text{Cs}_{0.5}\text{Rb}_{0.5}$ alloy

It is found that at the zone boundaries of [100] and [111] directions of high symmetry, i.e. for the larger momentum transfer the effects of local field correlations are almost negligible. These dispersion curves are not showing any abnormality in the three regions of high symmetry directions and are exhibiting qualitative behaviour like metallic elements.

REFERENCES

- Aditya M. Vora, *J. Phys. Chem. Sol.* **68**, 1725 (2007).
- Aditya M. Vora, *Chinese Phys. Lett.* **25**, 654 (2008).
- Aditya M. Vora, *Front. Mater. Sci. China* **2**, 311 (2008).
- Aditya M. Vora, *M. J. Condens. Matter.* **10**, 7 (2008).
- Aditya M. Vora, *Fizika A* **17**, 87 (2008).
- Aditya M. Vora, *The African Phys. Rev.* **4**, 95 (2010).
- Aditya M. Vora, *Armenian J. Phys. (Armenian Acad. Sci.)* **3**, 116 (2010).
- Aditya M. Vora, *J. Nano- Electron. Phys.* **3**, 5 (2011).
- P.N. Gajjar, M.H. Patel, B.Y. Thakore, A.R. Jani, *Commun. Phys.* **12**, 81 (2002).
- T. Soma, H. Ohsugi, H. Matsuo Kagaya, *phys. status. solidi b* **124**, 525 (1984).
- R.F. Wallis, A.A. Maradudin, A.G. Eguluz, A.A. Quong, A. Franchini, G. Santara, *Phys. Rev. B* **48**, 6043 (1993).
- W.A. Kamitakahara, J.R.D. Copley, *Phys. Rev. B* **18**, 3772 (1978).
- Y.A. Chushak, A. Baumketner, *Euro. Phys. J. B* **7**, 129 (1999).
- G. Jacussi, M.L. Klein, R. Taylor, *Phys. Rev. B* **18**, 3782 (1978).
- J. Hafner, *From Hamiltonians to Phase Diagrams*, (Heidelberg: Springer-Verlag: 1987)
- S. Ichimaru, K. Utsumi, *Phys. Rev. B* **24**, 7385 (1981).
- A. Sarkar, D.S. Sen, S. Haldar, D. Roy, *Mod. Phys. Lett. B* **12**, 639 (1998).
- W. Harrison, *Elementary Electronic Structure* (Singapore: World Scientific: 1999).

The phonon frequencies computed from IU-local field correction functions diverging from static H-function in [100] [111] and [100] directions of high symmetry are about 0% – 34.82%, 0% – 129.95%, 0% – 15.86% and 0% – 16.25% for $\text{Cs}_{0.5}\text{Li}_{0.5}$, $\text{Cs}_{0.5}\text{Na}_{0.5}$, $\text{Cs}_{0.5}\text{K}_{0.5}$ and $\text{Cs}_{0.5}\text{Rb}_{0.5}$ solid alloys, respectively. The phonon frequencies computed from S-local field correction functions differed from static H-function in [100], [111] and [100] of high symmetry directions are 0% – 99.27% for $\text{Cs}_{0.5}\text{Li}_{0.5}$, 0% – 148.73% for $\text{Cs}_{0.5}\text{Na}_{0.5}$, 0% – 99.39% for $\text{Cs}_{0.5}\text{K}_{0.5}$ and 0% – 13.22% for $\text{Cs}_{0.5}\text{Rb}_{0.5}$ solid solutions.

Also, we observed from the PDC that, when we move from $\text{Cs}_{0.5}\text{Li}_{0.5} \rightarrow \text{Cs}_{0.5}\text{Rb}_{0.5}$ alloys, the phonon frequency decreases with increase in the average volume of the solid alloys. The experimental phonon frequencies of such alloys are not available in the literature for further comparison and we find only few concrete remarks. But, in the absence of experimental information such calculations may be considered as one of the guidelines for further investigations either theoretical or experimental. Hence, such study could be extended for the other types of binary alloys. The relativistic effect of the heavier alkali element like Cs to other alkali elements is significant, but in the case of equiatomic alloys, this effect is comparatively small. Therefore, we have ignored relativistic effects of the heavier atom for the sake of simplicity.

4. CONCLUSIONS

We conclude that the present model is successful in explaining the static and vibrational properties of equiatomic Cs-based binary alloys and hence, it could be explored for predicting the behavior of other such solid solutions. The comparison of present theoretical findings helps us to note that the binding of $A_{1-x}B_x$ ($A = \text{Cs}$; $B = \text{Li, Na, K, Rb}$) is comparable to the pure metals, and hence, behaves like a solid metallic alloy. This can be confirmed by investigating its total crystal energy and heat of solution. Such study is under progress and the results will be reported in due course of the time. From the present experience, we also conclude that it should be interesting to apply other local pseudopotentials for such comprehensive study to judge and confirm the wider applicability of the potential.